MPMI Vol. 36, No. 3, 2023, pp. 176–188, https://doi.org/10.1094/MPMI-08-22-0165-R

A Novel Biosynthetic Gene Cluster Across the *Pantoea* Species Complex Is Important for Pathogenicity in Onion

Mei Zhao,[1,2] Gi Yoon Shin,[3] Shaun Stice,[3] Jonathon Luke Bown,[4] Teresa Coutinho,[5] William W. Metcalf,[4] Ron Gitaitis,[2] Brian Kvitko,[3] and Bhabesh Dutta[2,†]

[1] Department of Plant Pathology, College of Plant Protection, China Agricultural University, Beijing, P.R. China
[2] Department of Plant Pathology, University of Georgia, Tifton, GA, U.S.A.
[3] Department of Plant Pathology, University of Georgia, Athens, GA, U.S.A.
[4] Department of Microbiology, University of Illinois, Urbana-Champaign, IL, U.S.A.
[5] The Genomics Research Institute, University of Pretoria, Hatfield, South Africa

Accepted for publication 15 December 2022.

Onion center rot is caused by at least four species of genus *Pantoea* (*P. ananatis*, *P. agglomerans*, *P. allii*, and *P. stewartii* subsp. *indologenes*). Critical onion pathogenicity determinants for *P. ananatis* were recently described, but whether those determinants are common among other onion-pathogenic *Pantoea* species remains unknown. In this work, we report onion pathogenicity determinants in *P. stewartii* subsp. *indologenes* and *P. allii*. We identified two distinct secondary metabolite biosynthetic gene clusters present separately in different strains of onion-pathogenic *P. stewartii* subsp. *indologenes*. One cluster is similar to the previously described HiVir phosphonate biosynthetic cluster identified in *P. ananatis* and another is a novel putative phosphonate biosynthetic gene cluster, which we named Halophos. The Halophos gene cluster was also identified in *P. allii* strains. Both clusters are predicted to be phosphonate biosynthetic clusters based on the presence of a characteristic phosphoenolpyruvate phosphomutase (*pepM*) gene. The deletion of the *pepM* gene from either HiVir or Halophos clusters in *P. stewartii* subsp. *indologenes* caused loss of necrosis on onion leaves and red onion scales and resulted in significantly lower bacterial populations compared with the corresponding wild-type and complemented strains. Seven (*halB* to *halH*) of 11 genes (*halA* to *halK*) in the Halophos gene cluster are required for onion necrosis phenotypes. The onion nonpathogenic strain PNA15-2 (*P. stewartii* subsp. *indologenes*) gained the capacity to cause foliar necrosis on onion via exogenous expression of a minimal seven-gene Halophos cluster (genes *halB* to *halH*). Furthermore, cell-free culture filtrates of PNA14-12 expressing the intact Halophos gene cluster caused necrosis on onion leaves consistent with the presence of a secreted toxin. Based on the similarity of proteins to those with experimentally determined functions, we are able to predict most of the steps in Halophos biosynthesis. Together, these observations indicate that production of the toxin phosphonate seems sufficient to account for virulence of a variety of different *Pantoea* strains, although strains differ in possessing a single but distinct phosphonate biosynthetic cluster. Overall, this is the first report of onion pathogenicity determinants in *P. stewartii* subsp. *indologenes* and *P. allii*.

Keywords: Halophos, HiVir, *Pantoea allii*, *Pantoea stewartii* subsp. *indologenes*, *pepM*, phosphonate, toxin

Bacteria in the genus *Pantoea* are ubiquitous and form a wide range of interactions with eukaryotic hosts, including plants, fungi, insects, and humans (Coutinho and Venter 2009). Strains of at least four *Pantoea* species, *P. ananatis* (Gitaitis and Gay 1997), *P. agglomerans* (Edens et al. 2006; Hattingh and Walters 1981), *P. allii* (Brady et al. 2011), and *P. stewartii* subsp. *indologenes* (Stumpf et al. 2018), have been associated with onion center rot. Onion center rot can cause severe yield losses both in the field and in storage, and, in some cases, economic losses up to 90% have been experienced (Gitaitis and Gay 1997). In addition, recently, *P. dispersa* was reported to cause bulb decay of onion (Chang et al. 2018). Commercial onion cultivars with resistance to *Pantoea* spp. have not been identified (Stice et al. 2020). Thus, there is a need to understand pathogenesis mechanisms in *Pantoea* spp. that may potentially provide necessary information for future breeding efforts.

Two virulence factors that distinguish between onion-pathogenic and nonpathogenic strains of *P. ananatis* have recently been described (Asselin et al. 2018). Most bacterial pathogens depend on specialized virulence protein–based secretion systems for pathogenicity (Chang et al. 2014). Specifically, most gram-negative bacterial plant pathogens are dependent on either an *hrp* (hypersensitive response and pathogenicity) type III secretion system (T3SS) to deliver immune-dampening effector proteins or the type II secretion system (T2SS) to deliver the plant cell wall–degrading enzymes associated with soft rot diseases (Chang et al. 2014). The T3SS-mediated host-pathogen interactions have been extensively studied in *P. stewartii* subsp. *stewartii* and maize pathosystems (Roper 2011). *P. stewartii* subsp. *indologenes* also encodes a T3SS that shows the closest similarity to *P. stewartii* subsp. *stewartii hrp*-T3SS. However,

[†]Corresponding author: B. Dutta; bhabesh@uga.edu

Genome sequence data are available in the National Center for Biotechnology Information under the BioProject accession number PRJNA746326. The data that support the findings of this study are available from the corresponding author upon reasonable request.

Funding: Funding was provided by the National Institute of General Medical Sciences grant number R01 GM127659, National Institute of Food and Agriculture grant number 2019-51181-30013.

e-Xtra: Supplementary material is available online.

The author(s) declare no conflict of interest.

P. ananatis lacks T2SS and T3SS (De Maayer et al. 2014). Instead, *P. ananatis* requires a HiVir gene cluster for pathogenicity on onion (Asselin et al. 2018). Disruption of the HiVir cluster in *P. ananatis* resulted in the loss of pathogenicity on onion foliage, on scales of red onion bulbs, and on whole onion bulbs (Asselin et al. 2018; Polidore et al. 2021; Stice et al. 2020). The HiVir gene cluster was predicted to encode the synthesis of a phosphonate compound based on the presence of a characteristic *pepM* phosphoenolpyruvate (PEP) phosphonomutase gene within the cluster (Asselin et al. 2018). The novel phosphonate compound pantaphos (2-(hydroxy[phosphono]methyl)maleate) was shown to be synthesized by the HiVir cluster and is necessary and sufficient for the typical center rot symptom on onion (Polidore et al. 2021).

P. stewartii subsp. *indologenes* has long been known as a pathogen of pearl millet and foxtail millet (Mergaert et al. 1993). This pathogen was never associated with onion until recently, when it was reported in infected onion in the state of Georgia (Stumpf et al. 2018). Interestingly, only specific strains were able to cause disease on onion, which led to the proposition of two pathovars (Koirala et al. 2021). The epithet *P. stewartii* subsp. *indologenes* pv. *cepacicola* was proposed for strains (PNA03-3, PNA14-9, PNA14-11, and PNA14-12) that are pathogenic on *Allium* spp. including onion and, also, on foxtail millet, pearl millet, and oat (Koirala et al. 2021). Interestingly, the HiVir gene cluster was identified in the *P. stewartii* subsp. *indologenes* strain PNA03-3 but was absent in strains PNA14-9, PNA14-11, and PNA14-12 (Koirala et al. 2021). These observations were intriguing, as, despite the absence of the HiVir cluster, these strains were pathogenic on onion. We hypothesized that the HiVir gene cluster was important for PNA03-3 onion pathogenicity and that other pathogenicity factors could potentially be involved in onion pathogenicity in strains PNA14-9, PNA14-11, and PNA14-12. Hence, the objectives of this research were to identify and characterize pathogenicity and virulence factors in *P. stewartii* subsp. *indologenes* affecting onion and the role of T3SS in *P. stewartii* subsp. *indologenes*.

Results and Discussion

The presence of phosphonate biosynthetic gene clusters correlated with *P. stewartii* subsp. *indologenes* pathogenicity in onion.

Based on the annotation of secondary metabolite biosynthetic gene clusters, using antiSMASH 6.0 (Blin et al. 2021), we found that *P. stewartii* subsp. *indologenes* PNA14-12 (RefSeq assembly accession GCF_004364735.1) is predicted to possess a completely distinct putative phosphonate biosynthetic cluster. The strains that possess this putative gene cluster produced a pink halo around the necrotic tissue on red onion scales (Koirala et al. 2021), and hence, the name Halophos is being proposed here. To understand the onion pathogenicity mechanisms of *P. stewartii* subsp. *indologenes*, the genomes (under BioProject PRJNA676043) of onion-pathogenic strains and onion-nonpathogenic strains reported by Koirala et al. (2021) were analyzed for the presence of the HiVir and Halophos gene cluster sequences. Surprisingly, the phosphonate biosynthetic gene cluster HiVir was found only in PNA03-3 (Table 1). The Halophos gene cluster including a *pepM* homolog was identified in onion-pathogenic strains PNA14-9, PNA14-11, and PNA14-12 (Table 1). The phosphonate biosynthetic gene clusters (HiVir or Halophos) were present only in onion-pathogenic strains (PNA03-3, PNA14-9, PNA14-11, and PNA14-12), suggesting that the putative phosphonate compounds may potentially be essential for pathogenicity in onion. The Halophos cluster is adjacent to a phage/plasmid primase gene in *P. stewartii* subsp. *indologenes* PNA14-9, PNA14-11, and PNA14-12. The presence of the nearby primase gene suggests the Halophos cluster may have been acquired through horizontal gene transfer (HGT) (Hacker et al. 1997). The Halophos cluster from PNA14-12 is located within a genomic island predicted by IslandViewer 4 (Bertelli et al. 2017). In addition, the Halophos cluster has a lower percentage of guanine-cytosine (GC), higher average effective number of codons (Nc), and lower average codon adaptation index (CAI), compared with their corresponding whole genomes (Table 2). The Nc and CAI values are measures of synonymous codon usage bias (Sharp and Li 1987; Wright 1990). The higher Nc and lower CAI values in the Halophos gene cluster compared with the whole genome of

Table 2. Sequence signatures of Halophos gene cluster and PNA14-12 genome

Feature	Halophos gene cluster[a]	PNA14-12 genome[a]
Open reading frame GC content (%)	46.5 ± 2.9	53.5 ± 5.6
Effective number of codons	56.09 ± 2.39	46.36 ± 5.88
Codon adaptation index	0.25 ± 0.03	0.31 ± 0.08

[a] Values are averages ± standard deviation.

Table 1. *Pantoea stewartii* subsp. *indologenes* strains used for bioinformatic analysis to identify the Halophos gene cluster

Strain	RefSeq assembly accession	Onion pathogenicity[a]	Gene clusters	
			HiVir	Halophos
PNA 03-3	GCF_003201175.1	+	Present	Absent
PNA 14-9	GCF_017052375.1	+	Absent	Present
PNA 14-11	GCF_017052195.1	+	Absent	Present
PNA 14-12	GCF_004364735.1	+	Absent	Present
PNA 15-2	GCF_017052175.1	−	Absent	Absent
PANS 07-4	GCF_017052095.1	−	Absent	Absent
PANS 07-6	GCF_017052115.1	−	Absent	Absent
PANS 07-10	GCF_017051975.1	−	Absent	Absent
PANS 07-12	GCF_017052015.1	−	Absent	Absent
PANS 07-14	GCF_017051935.1	−	Absent	Absent
PANS 99-15	GCF_017051945.1	−	Absent	Absent
NCPPB 1562	GCF_017051845.1	−	Absent	Absent
NCPPB 1877	GCF_017051875.1	−	Absent	Absent
NCPPB 2275	GCF_017051895.1	−	Absent	Absent
NCPPB 2281	GCF_017051805.1	−	Absent	Absent
NCPPB 2282	GCF_017051815.1	−	Absent	Absent
LMG 2632	GCF_000757405.2	−	Absent	Absent

[a] + indicates positive reaction for onion pathogenicity and − indicates negative reaction for onion pathogenicity.

PNA14-12 implies recent acquisition via HGT event. In Georgia, onion and millet rotation were once recommended, and some organic onion growers still follow this rotation. We speculate that *P. stewartii* subsp. *indologenes* might have possibly horizontally acquired virulence factors from environmental or plant-associated microbes once associated with millet or other weeds capable of supporting onion-infecting bacteria as well as *P. stewartii* subsp. *indologenes* populations.

The Halophos gene cluster is predicted to contain 11 co-transcribed genes, which we have named *halA* through *halK*, putatively encoding one iron-containing alcohol dehydrogenase (*halA*), alcohol dehydrogenase (*halB*), *N*-acetyl-gamma-glutamyl-phosphate reductase (*halC*), phosphoglycerate dehydrogenase (*halD*), phosphoenolpyruvate mutase (*halE*), FAD-NAD(P)-binding protein (*halF*), aminotransferase (*halG*), phosphoglycerate kinase (*halH*), major facilitator superfamily (MFS) transporter (*halI*), AMP-binding enzyme (*halJ*), and pyridoxamine 5′-phosphate oxidase (*halK*) (Fig. 1). Notably, the *halJ* sequence is predicted to possess an adenylation domain and a condensation domain, suggesting that it might be involved in nonribosomal peptide synthetase activity.

Bioinformatics analysis of the Halophos-like gene clusters.

Analysis with antiSMASH predicted that the Halophos gene clusters of *P. stewartii* subsp. *indologenes* PNA14-12 and *P. allii* LMG24248 encode phosphonate secondary metabolite gene clusters. Using PNA14-12 Halophos nucleotide and protein sequences for blastn and tblastn searches, we identified 34 strains that encoded Halophos-like gene clusters (Supplementary Table S1). The strains belonged to genera *Pantoea*, *Erwinia*, *Pseudomonas*, *Xenorhabdus*, and *Photorhabdus*. *Pantoea allii* strains shared 85% sequence identity with the PNA14-12 Halophos nucleotide sequence. *Erwinia* strains shared 68 to 71% sequence identity with PNA14-12 Halophos nucleotide sequence. *Xenorhabdus*, *Photorhabdus*, and *Pseudomonas* spp. had 65 to 72% nucleotide sequence identity with the strain PNA14-12 Halophos sequence (at a sequence coverage of 30 to 46%) (Supplementary Table S1). Except for *Pseudomonas syringae* CC1557 (isolated from snow), all other strains that encoded Halophos-like sequences were isolated from plants or nematodes. *Xenorhabdus* and *Photorhabdus* species are nematode and arthropod symbionts. Interestingly, a HiVir-like cluster was also found in *Photorhabdus* spp. (Polidore et al. 2021). Many *Erwinia* and *Pseudomonas* species are common plant pathogens on various crops (Charkowski 2007; Coutinho and Venter 2009; Xin et al. 2018). Despite the presence of Halophos-like gene clusters in various bacterial genera, it would be interesting to test if this cluster contributes to bacterial virulence and survival under diverse hosts and environment.

The Halophos-like gene clusters displayed diversity in their synteny among different bacterial genera. When the Halophos-like cluster was compared between *Pantoea* and *Erwinia* strains, they showed the same gene synteny (Fig. 1B). The nematode endosymbiont genera *Xenorhabdus* and *Photorhabdus* do not contain *halI* (MFS transporter) and *halJ* (AMP-binding enzyme) in their Halophos-like gene clusters. The *halC* gene in *Xenorhabdus doucetiae* FRM16 was disrupted by a transposase

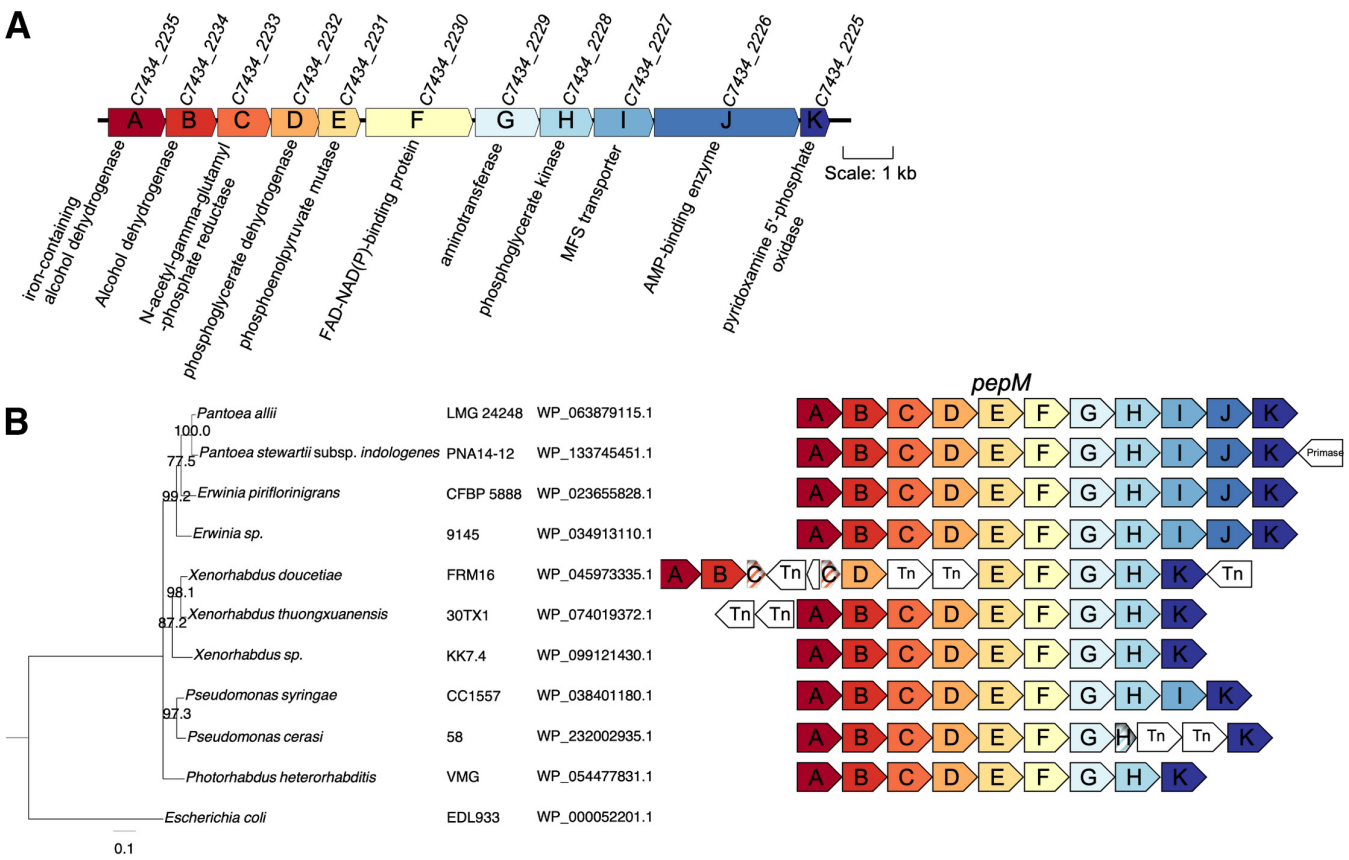

Fig. 1. Halophos gene cluster structure and synteny. **A,** Diagram of the Halophos gene cluster of *Pantoea stewartii* subsp. *indologenes* PNA14-12. The gene locus accessions are according to PNA14-12 annotation (accession NZ_SOAJ01000001). The scale represents 1 kb. **B,** A phylogenetic tree based on selected PepM protein sequences of organisms that have Halophos-like gene clusters. Ten PepM protein sequences and *Escherichia coli* 2-methylisocitrate lyase sequence (as an outgroup) were used for multiple sequence alignment, using MAFFT. The alignment was trimmed to the same length and was used for constructing a neighbor-joining tree. The bootstrap support values >70% are shown at the node. The conserved clusters (not to scale) are colored with the same colors representing homologous proteins. Nonconserved proteins are in white, and fragmented pseudogenes are in stripes. Transposase genes were labeled as Tn.

gene. Also, *Pseudomonas* strains do not have *halJ* in their gene clusters and *Pseudomonas cerasi* strains also have fragmented *halH* (Fig. 1B).

A comparison of the two phosphonate biosynthetic gene clusters, HiVir and Halophos, revealed that only two genes were similar based on predicted annotations, i.e., *pepM* and the MFS transporter gene. These *pepM* genes shared 35% amino acid identity. Both PepM proteins (HalE from Halophos and HvrA from HiVir) possessed the PEP mutase domain and the key PepM catalytic motif (EDKXXXXXNS). Similarly, the MFS transporter genes from the two phosphonate clusters shared 32% sequence identity. The MFS transporters from the HiVir and the Halophos gene clusters belonged to the macrolide efflux protein A family and the multidrug resistance protein MdtH family, respectively. These findings suggest their involvement in transporting different molecules.

The HiVir or Halophos gene cluster is critical for onion pathogenicity in *P. stewartii* subsp. *indologenes* but the T3SS is not.

The *pepM* gene is present in both phosphonate biosynthetic clusters (HiVir and Halophos) in *P. stewartii* subsp. *indologenes*. To decipher the role of *pepM* genes in these gene clusters, *pepM* was deleted, separately, in *P. stewartii* subsp. *indologenes* strains containing HiVir (PNA03-3) and Halophos (PNA14-12).

The *pepM* deletion mutant PNA03-3Δ*pepM* did not show the necrosis phenotype and had significantly lower population levels than the wild-type strain PNA03-3 on red onion scale and onion leaf tissues ($P < 0.0001$) (Fig. 2). Both bacterial load and necrosis phenotypes were complemented by the expression of the Halophos *pepM* gene (*halE*) from PNA14-12. Complementation of the PNA03-3 HiVir cluster *pepM* deletion with the *pepM* gene from PNA14-12 provides genetic validation that HalE is a functional PepM enzyme.

Deleting *hrcC*, the gene encoding the conserved T3SS outer membrane secretin, inactivates the T3SS (Charkowski et al. 1997). Interestingly, the *hrcC* deletion mutant did not result in phenotypic changes to population levels or onion disease symptoms in the deletion mutant (PNA03-3Δ*hrcC)* compared with wild-type strain PNA03-3. Overall, the results indicate that the *pepM* but not the *hrcC* gene is important for the onion pathogenicity in PNA03-3.

The deletion of the *pepM* gene in the Halophos gene cluster–containing *P. stewartii* subsp. *indologenes* strain (PNA14-12) resulted in significantly reduced population levels in the mutant (PNA14-12Δ*pepM*) compared with in the wild-type strain (PNA14-12 WT) on onion scale and leaf tissues (Fig. 3). The deletion mutant PNA14-12Δ*pepM* did not cause any lesion or necrosis on onion leaf and red onion scale (Fig. 3). In contrast, the wild-type strain (PNA14-12WT), the *hrcC* mutant (PNA14-12Δ*hrcC*), and the complemented strain (PNA14-12Δ*pepM* pBS46::$pepM_{14\text{-}12}$) showed distinct pink halo phenotypes (Fig. 3). These lesions were distinct from those that are caused by typical HiVir gene cluster–containing *Pantoea* spp. strains, as observed in *P. ananatis* PNA97-1 (white clearing zone without halo) (Stice et al. 2020). Similar to *P. stewartii* subsp. *indologenes* PNA03-3, deletion of the *hrcC* gene in *P. stewartii* subsp. *indologenes* PNA14-12 did not result in phenotypic changes to population levels or necrosis phenotype compared with the wild-type strain. This indicated that *pepM* in the Halophos gene

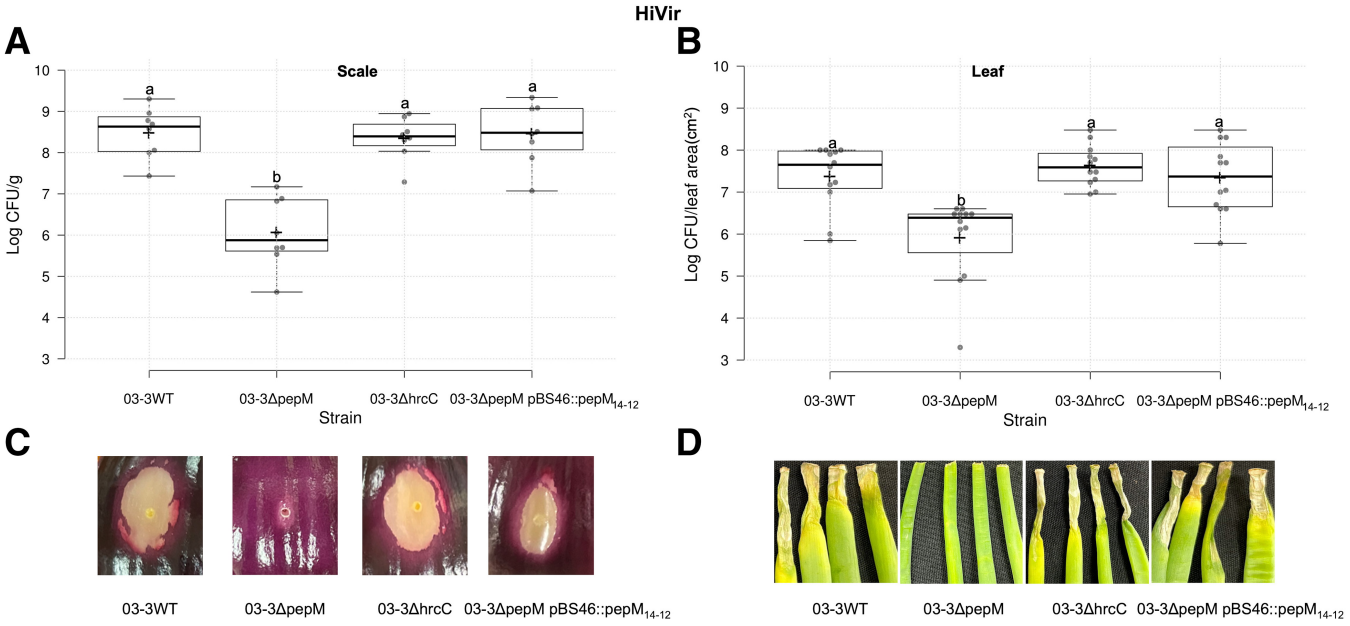

Fig. 2. A *pepM* (HiVir) deletion mutant in *Pantoea stewartii* subsp. *indologenes* PNA03-3 became nonpathogenic in onions and was complemented using *pepM* from the *P. stewartii* subsp. *indologenes* PNA14-12 Halophos gene cluster. **A,** Bacterial populations in onion scale and **B,** leaf tissues inoculated with *P. stewartii* subsp. *indologenes* PNA03-3 wild type (WT) and mutants. **C,** Representative symptoms produced on red onion scales (cv. Red Barret) and **D,** 6-week-old onion leaves (cv. Century). PNA03-3 WT, 03-3Δ*pepM* mutant, 03-3Δ*hrcC* mutant, and 03-3Δ*pepM* pBS46::$pepM_{14\text{-}12}$ complemented strains were inoculated onto red onion scales and leaves at 10^4 colony-forming units (CFU) ($n = 4$) (A, B, and D) or 10^6 CFU (C). Samples and images were taken 4 days postinoculation. For the onion scale necrosis assay, tissue samples (0.2 × 0.2 cm) were taken 0.5 cm away from the inoculation point, were weighed, were macerated in sterilized H_2O, and were plated on Luria-Bertani agar with rifampicin. Colonies were counted 24 h after incubation and numbers were converted to Log_{10} CFU per gram. For onion leaf inoculation assays, samples (0.5 cm long) were taken 0.3 cm away from the inoculation point, were processed similarly to the scale samples, and the colonies were enumerated as Log_{10} CFU per square centimeter of leaf area. Center lines show the medians; box limits indicate the 25th and 75th percentiles; whiskers extend up to the furthermost data point that falls within 1.5 times the interquartile range from the 25th and 75th percentiles; crosses represent sample means; data points are plotted as gray circles, as determined by R software. Sample points $n = 8$ and 12 are shown for graphs A and B, respectively. Different letters indicate significant differences ($P = 0.05$) among treatments, according to Tukey-Kramer's honestly significant difference test. Complementation of the PNA03-3 HiVir cluster *pepM* deletion with the *pepM* gene from PNA14-12 provides genetic validation that HalE is a functional PepM enzyme.

cluster is important for onion pathogenicity in PNA14-12. Also, the *hrcC* gene in the T3SS does not contribute to onion pathogenicity.

Based on the initial nucleotide sequence similarity search of the Halophos gene cluster, we found that another onion pathogen, *P. allii* LMG24248, also contains the entire gene cluster with complete synteny (Fig. 1; Supplementary Table S1). Further, the role of *pepM* gene in the Halophos cluster from *P. allii* LMG24248 was investigated. The deletion mutant *P. allii* LMG24248Δ*pepM* had significantly lower population levels than the LMG24248 wild type in onion scale and leaf tissues ($P < 0.0001$). The deletion mutant (LMG24248Δ*pepM*) also did not display symptoms on red onion scales and on onion leaves (Fig. 4). Both bacterial population levels and symptoms were complemented by the expression of the Halophos *pepM* gene (*halE*) from LMG24248 (Fig. 4). This indicated that *pepM* gene in the Halophos gene cluster of *P. allii* is also important for onion pathogenicity, which has never been demonstrated experimentally previously. We also note that none of the *P. allii* strain sequences investigated in this study (LMG24248, BD381, BD382, BD383, BD386, BD387, BD388, and BD389) encoded T3SS; however, T3SS was present in *P. stewartii* subsp. *indologenes*.

We sequenced seven additional *P. allii* strains (BD381, BD382, BD383, BD386, BD387, BD388, and BD389) isolated from onion in South Africa. Based on whole-genome sequencing, all seven *P. allii* strains encoded the Halophos-like gene cluster and their gene content and gene orientations within the cluster were identical. All seven strains caused foliar necrosis upon inoculation in onion leaf and displayed pink halo phenotypes in the red onion scale assays (Supplementary Fig. S2).

The *hal* genes (Halophos) contribute to the pathogenicity of *P. stewartii* subsp. *indologenes* PNA14-12 in onion.

In order to determine the roles of other genes besides *pepM/halE* in the Halophos gene cluster, we made single mutants of each Halophos gene in PNA14-12, inoculated them on onion scales and leaves, and assessed the symptoms at 5 days postinoculation (dpi). The strains *P. stewartii* subsp. *indologenes* PNA14-12WT, Δ*halA*, Δ*halI*, Δ*halJ*, and Δ*halK* showed distinct pink halo phenotypes on the red onion scales and caused necrosis on onion leaf, while Δ*halB*, Δ*halC*, Δ*halD*, Δ*halF*, and Δ*halG* did not display any symptoms on the red onion scales and on onion leaves (Fig. 5A and B). The Δ*halH* deletion mutant showed no symptoms on the red onion scales but showed reduced foliar necrosis (Fig. 5A and B). The complemented strains of *halB*, *halC*, *halD*, *halF*, *halG*, and *halH* showed pink halo phenotypes and foliar necrosis (Fig. 5A and B). The deletion mutant strains Δ*halB*, Δ*halC*, Δ*halD*, Δ*halF*, and Δ*halG* displayed no lesion (Fig. 5C), while the mean lesion length for Δ*halH* was significantly shorter than that for 14-12WT, Δ*halA*, Δ*halI*, Δ*halJ*, and Δ*halK*. The complemented strains, *halBcomp*, *halC*comp, *halD*comp, *halF*comp, *halG*comp, and *halH*comp, showed significantly longer mean lesion length than that of their corresponding mutant strains ($P < 0.0001$) (Fig. 5C). The results indicate that *halB-H* but not *halA*, *halI*, *halJ*, *halK* genes contribute to onion pathogenicity. To our surprise, *halI*, the MFS transporter gene from the Halophos gene cluster, did not contribute to onion pathogenicity (Fig. 5), while *hvrI*, the MFS transporter gene from the HiVir cluster in *P. ananatis*, was shown to be important for onion foliar necrosis (Asselin et al. 2018). We speculate that PNA14-12 does not rely on *halI* but other unknown means to transport its product of Halophos out of the cell.

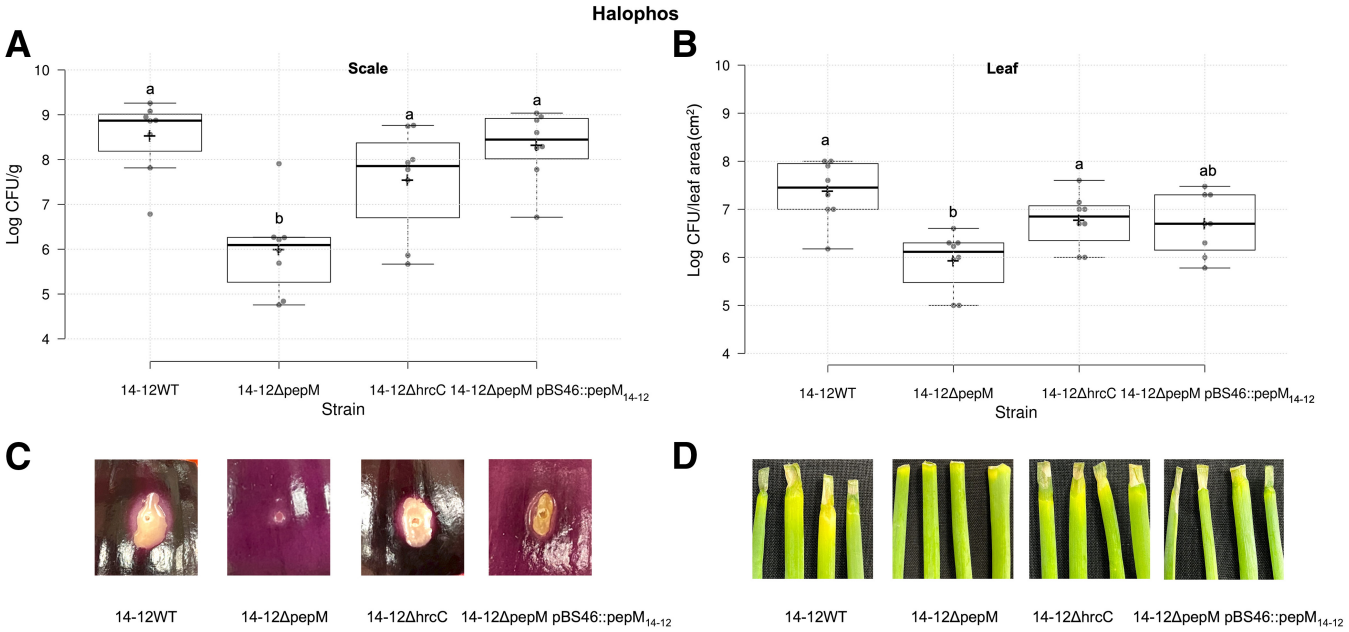

Fig. 3. The *pepM* (from Halophos) is vital for *Pantoea stewartii* subsp. *indologenes* PNA14-12 pathogenicity on onion scale and leaf. **A,** Bacterial population levels in onion scale and **B,** leaf tissues inoculated with *P. stewartii* subsp. *indologenes* PNA14-12 wild type (WT) and mutants. **C,** Representative symptoms produced on red onion scales (cv. Red Barret) and **D,** 6-week-old onion leaves (cv. Century). PNA14-12 WT, 14-12Δ*pepM* mutant, 14-12Δ*hrcC* mutant, and 14-12Δ*pepM* pBS46::*pepM*$_{14\text{-}12}$ complemented strains were inoculated onto red onion scales and leaves at 10^4 colony-forming units (CFU) ($n = 4$) (A, B, and D) and 10^6 CFU (C). Samples and images were taken 4 days postinoculation. For the onion scale necrosis assay, tissue samples (0.2 × 0.2 cm) were taken 0.5 cm away from the inoculation point, were weighed, were macerated in sterilized H_2O, and were plated on Luria-Bertani agar with rifampicin. Colonies were counted 24 h after incubation and numbers were converted to Log_{10} CFU per gram. For onion leaf inoculation assays, samples (0.5 cm long) were taken 0.3 cm away from the inoculation point, were processed similarly to the scale samples, and the colonies were enumerated as Log_{10} CFU per square centimeter of leaf area. Center lines show the medians; box limits indicate the 25th and 75th percentiles; whiskers extend up to the furthermost data point that falls within 1.5 times the interquartile range from the 25th and 75th percentiles; crosses represent sample means; data points are plotted as gray circles, as determined by R software. The experiment was conducted twice and all sample points ($n = 8$) are shown. Different letters indicate significant differences ($P = 0.05$) among treatments, according to Tukey-Kramer's honestly significant difference test.

The segment of seven contiguous *hal* genes (*halB to halH*) was expressed in onion-nonpathogenic strain *P. stewartii* subsp. *indologenes* PNA15-2. On onion leaves, the wild-type *P. stewartii* subsp. *indologenes* PNA15-2 (lacks Halophos) did not cause foliar necrosis, while the transformant PNA15-2 pBS46::*halB-H* induced limited necrotic lesions (Fig. 5D and E). We showed that by transferring a minimal cluster of *halB to halH* to an onion-nonpathogenic strain, PNA15-2, the strain was able to cause foliar necrosis on onion. Furthermore, necrosis was not observed on onion scales at 5 dpi for strain PNA15-2 and its transformant, PNA15-2 pBS46::*halB-H*. We speculate that the underlying reason could be attributed to the low expression level of the plasmid carrying a large fragment of *halB to halH* (8,614 bp). Alternatively, it is also possible that other components could be present in PNA14-12 but absent in PNA15-2 that might be needed to facilitate its expression. It is also possible that yet-to-determined regulators outside the cluster might regulate its expression that resulted in reduced phenotype. A further detailed investigation may shed some light in the future.

On the other hand, only *pepM* and the MFS transporter gene from the HiVir cluster were previously characterized and shown to be important for onion pathogenicity (Asselin et al. 2018; Polidore et al. 2021; Stice et al. 2020). The individual contributions of other genes in the HiVir cluster remain to be determined. Identifying the minimal number of genes required for phosphonate biosynthesis may help in the identification of key players involved in the biosynthetic pathway and may aid in understanding how phosphonates are synthesized.

Bacterial culture filtrate induced symptoms on onion leaves.

We generated a derivative strain of *P. stewartii* subsp. *indologenes* PNA14-12 to express the Halophos cluster under the control of the P*rhaB* promoter. The scheme is depicted in Supplementary Figure S3 and is similar to the scheme used to express pantaphos used by Polidore et al. 2021. When cultured with rhamnose supplementation, the filtered culture supernatant of strain PNA14-12WT pSC201::*halA* and the strain PNA14-12Δ*pepM* pSC201::*halA* pBS46::*pepM* induced necrosis on onion leaves, while strain PNA14-12 Δ*pepM* pSC201::*halA* did not (Fig. 6). When cultured without rhamnose supplementation, the culture supernatant of all three strains did not cause any symptoms (Fig. 6). These observations indicate that the product produced by the Halophos gene cluster is a potential toxin and can induce necrosis similar to that caused by a live *P. stewartii* subsp. *indologenes*.

Predicted biosynthetic pathway for the production of Halophos.

Based on the similarity of proteins encoded by the Halophos gene cluster to those with experimentally determined functions, we are able to predict most of the steps in Halophos biosynthesis (Supplementary Fig. S4). The first five steps in this putative biosynthetic pathway are identical to those in the recently characterized valinophos pathway (Ju et al. 2015; Zhang et al. 2022). According to the prediction, PEP is predicted to be converted into 2,3-dihydroxypropylphosphonic acid (DHPPA) by the sequential action of HalE, HalD, HalH, HalC, and HalA, which are homologs of the valinophos biosynthetic

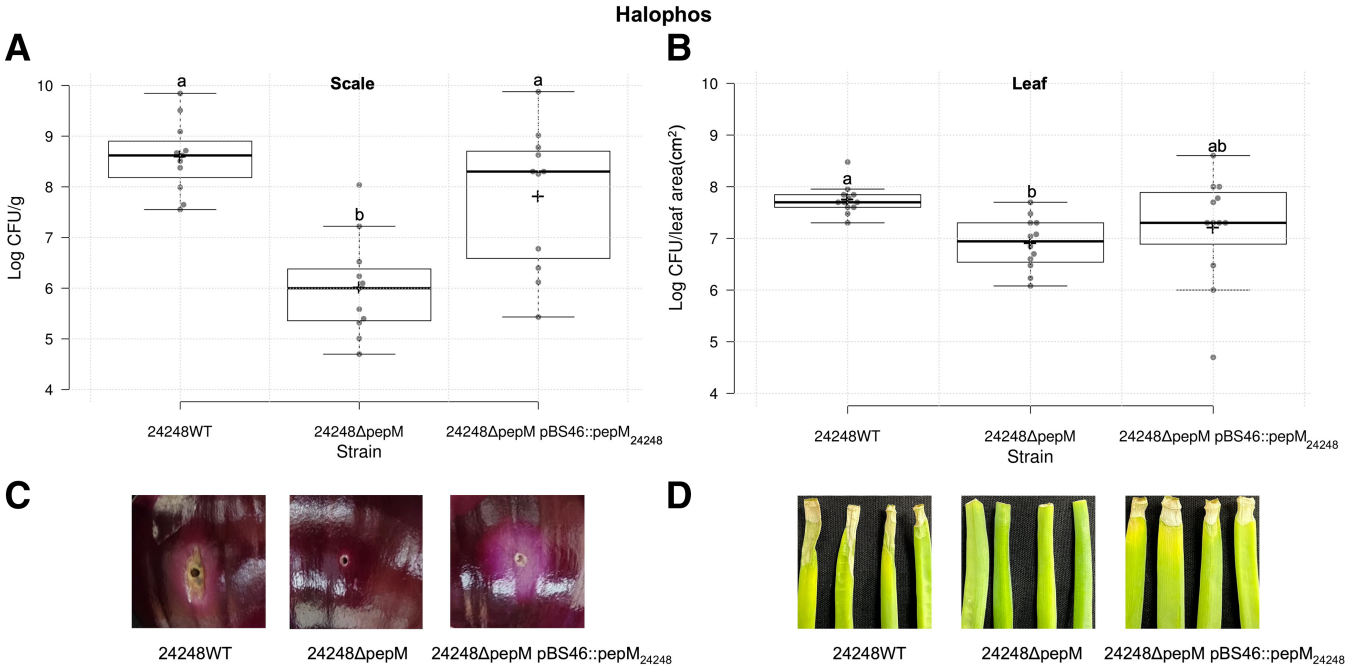

Fig. 4. The *pepM* (from Halophos) is vital for *Pantoea allii* LMG24248 pathogenicity on onion scale and leaf. **A,** Bacterial population levels in onion scale and **B,** leaf tissues inoculated with *P. allii* LMG24248 wild type and mutants. **C,** Representative symptoms produced on red onion scales (cv. Red Barret) and **D,** 6-week-old onion leaves (cv. Century). The 24248 wild-type (WT), 24248Δ*pepM* mutant, and 24248Δ*pepM* pBS46::$pepM_{24248}$ complemented strains were inoculated onto red onion scales and leaves at 10^4 CFU ($n = 4$) (A, B, and D) and 10^6 CFU (C). Samples and images were taken 4 days postinoculation. For the onion scale necrosis assay, tissue samples (0.2 × 0.2 cm) were taken 0.5 cm away from the inoculation point, were weighed, were macerated in sterilized H_2O, and were plated on Luria-Bertani agar with rifampicin. Colonies were counted 24 h after incubation and numbers were converted to Log_{10} colony-forming units per gram. For onion leaf inoculation assays, samples (0.5 cm long) were taken 0.3 cm away from the inoculation point, processed similarly to the scale samples, and the colonies were enumerated as Log_{10} CFU per square centimeter of leaf area. Center lines show the medians; box limits indicate the 25th and 75th percentiles; whiskers extend up to the furthermost data point that falls within 1.5 times the interquartile range from the 25th and 75th percentiles; crosses represent sample means; data points are plotted as gray circles, as determined by R software. The experiment was conducted three times and all sample points ($n = 12$) were shown. Different letters indicate significant differences ($P = 0.05$) among treatments, according to Tukey-Kramer's honestly significant difference test.

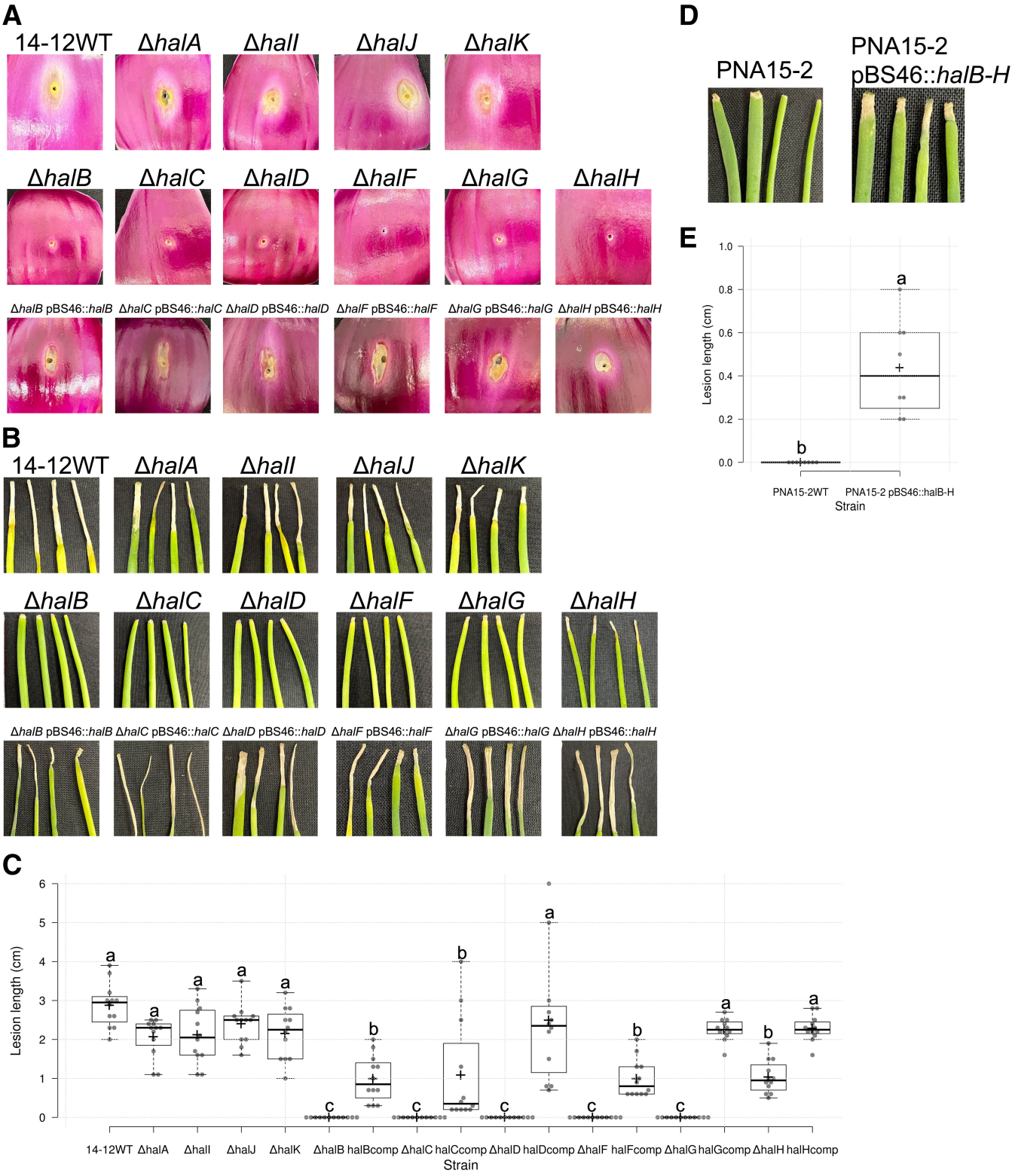

Fig. 5. The *halB-H* genes are critical for *Pantoea stewartii* subsp. *indologenes* PNA14-12 and PNA15-2 pathogenicity on onion. **A,** Representative symptoms produced on red onion scales (cv. Red Barret) and **B,** 6-week-old onion leaves (cv. Century). PNA14-12 wild type (WT), *hal* mutants, and *hal* complemented strains were inoculated onto red onion scales and leaves at 10^6 CFU ($n = 4$). Samples and images were taken 5 days postinoculation (dpi). **C,** Lesion length on onion leaf. Complemented strains are noted as halXcomp. Center lines show the medians; box limits indicate the 25th and 75th percentiles; whiskers extend up to the furthermost data point that falls within 1.5 times the interquartile range from the 25th and 75th percentiles; crosses represent sample means; data points are plotted as gray circles, as determined by R software. All sample points are shown ($n = 12$ and 8 [C and E, respectively]). Different letters indicate significant differences ($P = 0.05$) among treatments, according to Tukey-Kramer's honestly significant difference test. **D,** PNA15-2 and PNA15-2 pBS46::*halB-H* strains were inoculated onto onion leaves at 10^6 CFU ($n = 4$) and **E,** lesion length of onion leaf ($n = 8$). Samples and images were taken at 5 dpi.

enzymes VlpA (40% identity), VlpB (39% identity), VlpD (29% identity), VlpC (42% identity), and VlpE (28% identity), respectively. HalB is not closely related to characterized phosphonate biosynthetic enzymes; nevertheless, it is clearly a member of the medium chain dehydrogenases/reductase alcohol dehydrogenase family (Persson et al. 2008), which are known to oxidize secondary alcohols to ketones. Thus, we predict that HalH might oxidize DHPPA to (3-hydroxy-2-oxopropyl) phosphonate (HOPPA). The HOPPA is predicted to be converted to (2-amino-3-hydroxypropyl) phosphonate (AHPPA) via the transaminase HalG. Finally, as a homolog of the characterized amine oxidase HpxL involved in phosphonocystoximic acid biosynthesis (Goettge et al. 2018), we predict that HalF might oxidize AHPPA to the corresponding oxime. This putative pathway accounts for eight of the 11 *hal* operon genes; however, one caveat is that the predictions are inferred based on sequence homology, and their functions have not been experimentally validated in *Pantoea* spp. The remaining proteins include HalJ, which encodes an adenylation domain protein, and HalK, a member of the flavin-dependent pyrodoxamine-phosphate oxidase family. We are currently unable to predict functions for these proteins; thus, the final structure of Halophos cannot easily be predicted. The final unassigned gene is HalI, a member of the MFS, is predicted to be responsible for export of the final phosphonate product. The unaccounted-for genes in the prediction of Halophos production, *halI*, *halJ*, and *halK*, also seem to be dispensable based on mutational analysis data.

The *hrcC* but not the *pepM* gene is important for the pathogenicity of *P. stewartii* subsp. *indologenes* on millet.

The T3SS genes of *P. stewartii* subsp. *indologenes* show 97.6% nucleotide sequence identity to T3SS genes of *P. stewartii* subsp. *stewartii* and the two subspecies share similar T3SS gene organization (Supplementary Fig. S5). The *P. stewartii* subsp. *stewartii hrp* T3SS is essential to elicit hypersensitive response (HR) in tobacco and *Nicotiana benthamiana* and to cause disease in maize (Coplin et al. 1992a and b; Ham et al. 2008). The *P. stewartii* subsp. *indologenes* strains PNA 03-3 and PNA 14-12 possess two type III secreted effectors (T3SE) (AvrB3 (PXV73943.1 of PNA 03-3, TDS67862.1 of PNA 14-12) and WtsE (PXV73945.1 of PNA 03-3, TDS67864.1 of PNA14-12)), while the *P. stewartii* subsp. *stewartii* DC283 strain encodes genes for five plant-associated T3SE (WtsE [ARF52487.1], HopE1 [ARF52716.1], Eop3 [ARF52720.1], HopC1 [truncated; locus tag *DSJ_26290*], and HopAM1 [truncated; ARF52484.1, ARF52485.1]). The role of these *P. stewartii* subsp. *indologenes* effectors in millet pathogenicity is yet to be elucidated; however, in this manuscript, we demonstrated that the *hrp* T3SS plays a critical role in pathogenicity in millet. Pathogenicity was lost when *hrcC*, which encodes a core component of the T3SS, was deleted.

On pearl millet leaves, the *hrcC* deletion mutant (PNA03-3Δ*hrcC*) reached significantly lower population levels than the wild-type strain (PNA03-3WT), the *pepM* (in HiVir cluster) deletion mutant strain (PNA03-3Δ*pepM*), and the complemented strain (PNA03-3Δ*hrcC* pBS46::$hrcC_{03\text{-}3}$) at 4 dpi ($P < 0.0001$) (Fig. 7A). The strains PNA03-3WT, PNA03-3Δ*pepM*, and PNA03-3Δ*hrcC* pBS46::$hrcC_{03\text{-}3}$ developed obvious lesions, while PNA03-3Δ*hrcC* did not develop any symptoms on inoculated pearl millet leaves (Fig. 7B). Similarly, deletion of *hrcC* gene from the Halophos-containing strain (PNA14-12) did affect its pathogenicity on pearl millet. The deletion mutant PNA14-12Δ*hrcC* reached significantly lower population levels than PNA14-12WT, *pepM* (in Halophos cluster) deletion mutant strain PNA14-12Δ*pepM*, and the complemented strain (PNA14-12Δ*hrcC* pBS46::$hrcC_{03\text{-}3}$) at 4 dpi ($P < 0.0001$) (Fig. 7C). The strains PNA14-12WT, PNA14-12Δ*pepM*, and PNA14-12Δ*hrcC* pBS46::$hrcC_{03\text{-}3}$ developed obvious lesions, while PNA14-12Δ*hrcC* did not develop any symptoms on inoculated pearl millet leaves (Fig. 7D). We showed, for the first time, the importance of *P. stewartii* subsp. *indologenes* T3SS on millet pathogenicity.

P. stewartii subsp. *indologenes* may utilize T3SS to colonize and infect millets, but, on onion, it may utilize a different set of pathogenicity factors, HiVir or Halophos, which results in host cell death. These observations potentially suggest that onion-pathogenic *P. stewartii* subsp. *indologenes* may utilize different pathogenicity factors preferentially when they are present on millet vs. on onion. Future detailed studies may shed some light on their importance in host-range expansion.

Importance of *hrcC* and *pepM* genes in the tobacco hypersensitive-like cell death response.

Many plant-pathogenic bacteria use secretion systems to deliver proteins to plant cell targets and these secretion systems are often associated with plant pathogenicity and vir-

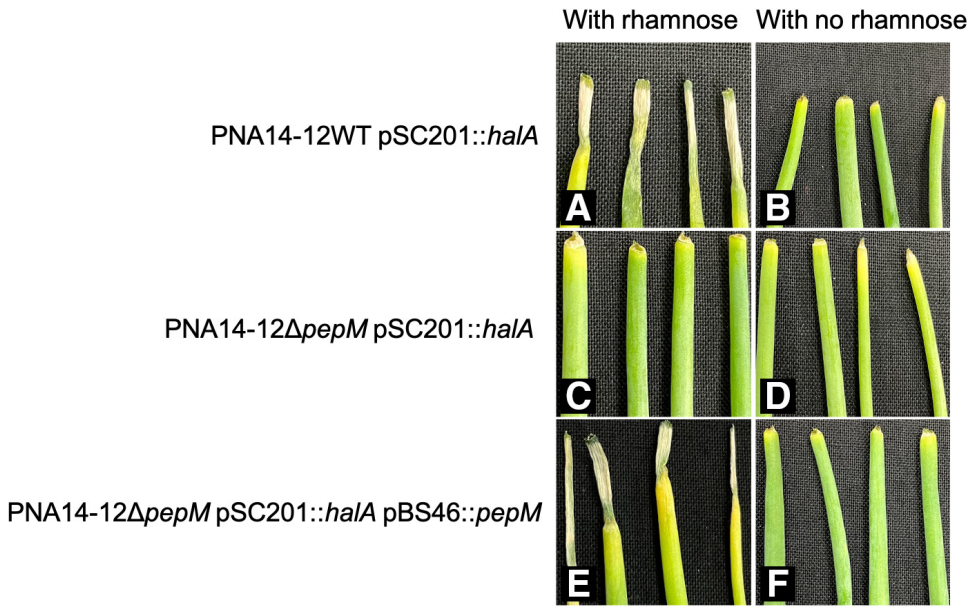

Fig. 6. Cell-free culture filtrate induced symptoms on onion leaf. Bacteria were grown in modified Coplin lab medium (mCLM) for 24 h and were centrifuged. The supernatant was filtered and 20 µl was inoculated onto the cut onion leaf tip. Images were taken 4 days postinoculation. **A,** PNA14-12WT pSC201::*halA* in mCLM + trimethoprim + rhamnose; **B,** PNA14-12WT pSC201::*halA* in mCLM + trimethoprim; **C,** PNA14-12Δ*pepM* pSC201::*halA* in mCLM + trimethoprim + rhamnose; **D,** PNA14-12Δ*pepM* pSC201::*halA* in mCLM + trimethoprim; **E,** PNA14-12Δ*pepM* pSC201::*halA* pBS46::*pepM* in mCLM + gentamicin + trimethoprim + rhamnose; **F,** PNA14-12Δ*pepM* pSC201::*halA* pBS46::*pepM* in mCLM + gentamicin + trimethoprim. Experiments were conducted twice with similar results.

ulence (Chang et al. 2014). HR assays were assessed on tobacco to determine the function of T3SS in *P. stewartii* subsp. *indologenes*. We also evaluated if the products from the HiVir and Halophos clusters in *Pantoea* spp. (*P. stewartii* subsp. *indologenes* and *P. allii*) induced cell-death responses on tobacco. Leaves infiltrated with the suspensions of *P. stewartii* subsp. *indologenes* PNA03-3WT, PNA03-3Δ*hrcC*, PNA03-3Δ*pepM*, PNA03-3Δ*hrcC* pBS46::$hrcC_{03\text{-}3}$, PNA03-3Δ*pepM*Δ*hrcC* pBS46::$hrcC_{03\text{-}3}$, and PNA03-3Δ*pepM*Δ*hrcC* pBS46::$pepM_{14\text{-}12}$ developed cell death after 48 h (Fig. 8A). The double mutant PNA03-3Δ*pepM*Δ*hrcC* could not induce cell death (Fig. 8A). Leaves infiltrated with suspensions of PNA14-12WT, PNA14-12Δ*pepM*, PNA14-12Δ*hrcC* pBS46::$hrcC_{03\text{-}3}$, PNA14-12Δ*pepM*Δ*hrcC* pBS46::$hrcC_{03\text{-}3}$ developed cell death after 48 h (Fig. 8B). Leaves infiltrated with PNA14-12Δ*hrcC*, PNA14-12Δ*pepM*Δ*hrcC*, and the control did not induce cell death (Fig. 8B). Leaves infiltrated with suspensions of *P. allii* 24248WT, 24248Δ*pepM*, 24248Δ*pepM* pBS46::$pepM_{24248}$, and the control did not induce cell death (Fig. 8C). It is interesting to note that PNA03-3Δ*hrcC* caused cell death but PNA03-3Δ*pepM*Δ*hrcC*, PNA14-12Δ*hrcC*, and *P. allii* LMG24248WT did not, suggesting the HiVir toxin from PNA03-3 but not the Halophos toxins from PNA14-12 and *P. allii* LMG24248 is toxic to tobacco leaf (Fig. 8). This also indicates the modes of action between HiVir and Halophos products are potentially different. We also noted that the cell death induced by PNA03-3Δ*hrcC* was delayed compared with PNA03-3WT and PNA03-3Δ*pepM* at 24 h but was similar at 48 h (Supplementary Fig. S6).

The products of the predicted phosphonate biosynthetic cluster we named Halophos and their biological functions are currently unknown. Understanding the products, the regulation of phosphonate biosynthesis, and the synthetic stages may help provide targets for developing specific enzyme inhibitors against plant-pathogenic *Pantoea* spp. carrying Halophos. In conclusion, a unique gene cluster, Halophos, responsible for onion tissue necrosis was found in *P. stewartii* subsp. *indologenes* and also in *P. allii*. We characterized the genes in this cluster and demonstrated that seven of the 11 genes are required for onion necrosis phenotypes. Also, the expression of the Halophos cluster conferred onion foliar necrosis phenotype similar to those produced by a live *P. stewartii* subsp. *indologenes*. Based on the similarity of proteins to those with experimentally determined functions, we predict most of the steps in Halophos biosynthesis. Future research on Halophos structure and its target are needed for developing strategies to manage *Pantoea* spp. in onion. The elucidation of the Halophos structure will be performed using standardized techniques for detecting phosphonate compounds. Nuclear magnetic resonance (NMR) spectroscopy, especially ^{31}P NMR can be used to characterize the compounds. Modern liquid chromatography–mass spectrometry techniques can also be applied to facilitate compound identification.

Materials and Methods

Bacterial strains and inoculum preparation.

Bacterial strains and plasmids used in the study are listed in Supplementary Table S2. Naturally occurring, rifampicin-resistant strains of representative *Pantoea* strains were selected. *Pantoea* strains were routinely cultured on nutrient agar at 28°C for 1 day and *Escherichia coli* strains on Luria-Bertani broth or agar at 37°C for 1 day. When required, media were supplemented with kanamycin at 50 μg/ml, trimethoprim at 100 μg/ml, gentamycin at 20 μg/ml, X-gluc at 60 μg/ml, rifampicin at 50 μg/ml, and diaminopimelic acid (DAP) for *E. coli* RHO5 at 300 μg/ml. To prepare *Pantoea* inocula, strains were cultured

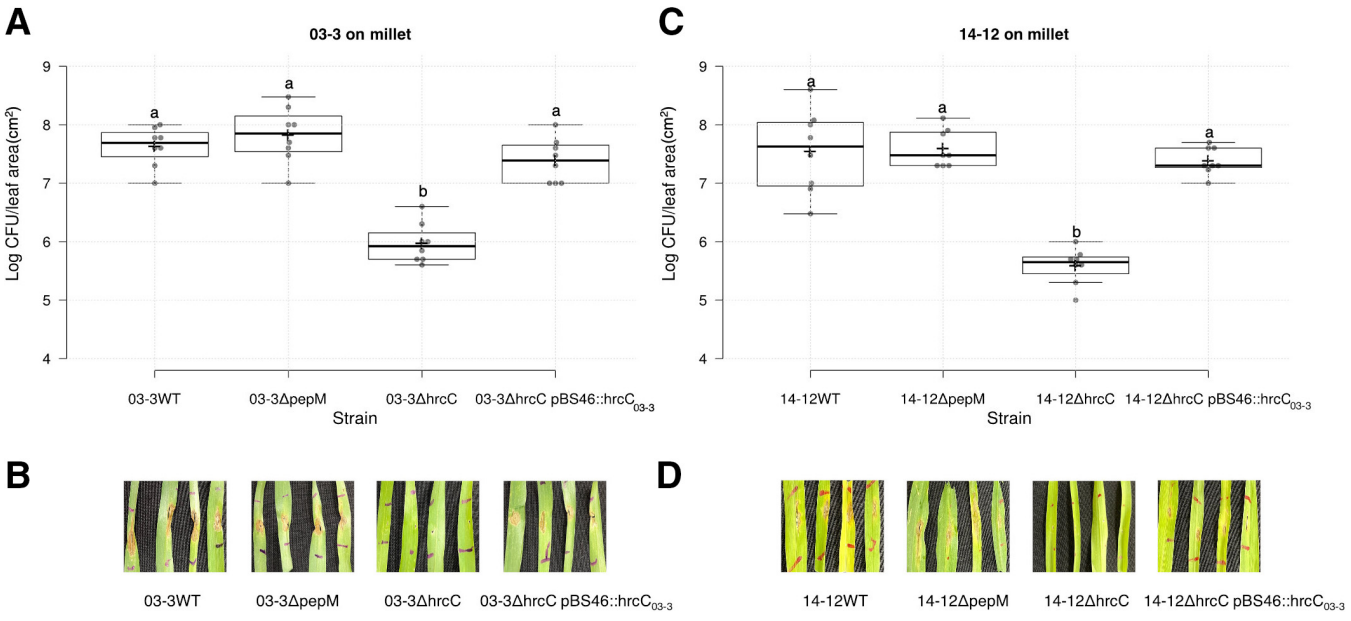

Fig. 7. The *hrcC* gene is vital for PNA03-3 and PNA14-12 pathogenicity on pearl millet. **A and C,** Bacterial population levels in millet tissues inoculated with *Pantoea stewartii* subsp. *indologenes* PNA03-3 and PNA14-12 wild type (WT) and mutants. **B and D,** Representative symptoms produced by 4-week-old millet leaves. PNA03-3 WT, 03-3Δ*pepM* mutant, 03-3Δ*hrcC* mutant, and 03-3Δ*hrcC* pBS46::$hrcC_{03\text{-}3}$ complemented strains, PNA14-12 WT, 14-12Δ*pepM* mutant, 14-12Δ*hrcC* mutant, and 14-12Δ*hrcC* pBS46::$hrcC_{03\text{-}3}$ complemented strains were inoculated into millet leaves at 10^6 CFU/ml. Samples and images were taken 4 days postinoculation. Two leaf disks (0.4 cm diameter) were sampled from four leaves, were macerated in sterilized H_2O, and were plated on Luria-Bertani agar with rifampicin. The colonies were counted 24 h after incubation and the number converted to Log_{10} CFU per square centimeter of leaf area. Center lines show the medians; box limits indicate the 25th and 75th percentiles; whiskers extend up to the furthermost data point that falls within 1.5 times the interquartile range from the 25th and 75th percentiles; crosses represent sample means; data points are plotted as gray circles, as determined by R software. The experiment was conducted twice, and all sample points ($n = 8$) are shown. Different letters indicate significant differences ($P = 0.05$) among treatments, according to Tukey-Kramer's honestly significant difference test.

in Luria-Bertani (LB) at 28°C, in a rotary shaker at 200 rpm, for approximately 16 h. Subsequently, the cultures were centrifuged at 16,100 × *g* for 1 min and the supernatants were decanted. The resulting pellets were resuspended in sterilized distilled water (sdH_2O). The bacterial concentrations were then adjusted to an optical density of 0.3 at 600 nm (about 10^8 colony-forming units per milliliter [CFU/ml]), using a spectrophotometer, and were adjusted to the desired concentration by 10-fold serial dilutions in sdH_2O.

Mutant constructions.

To determine the role of *pepM* in *Pantoea* pathogenicity, unmarked deletions of *pepM* gene in *P. allii* LMG24248 and *P. stewartii* subsp. *indologenes* PNA03-3 and PNA14-12 were made, using the pR6KT2GW allelic exchange vector, following the method described by Stice et al. 2020, and were named 24248Δ*pepM*, PNA03-3Δ*pepM*, and PNA14-12Δ*pepM*, respectively. The primers used are listed in Supplementary Table S3. Double-stranded DNA containing the *pepM* flanking sequences were synthesized (Twist Biosciences, San Francisco) and are listed in Supplementary Table S4. Mutants were confirmed by PCR and Sanger sequencing. To determine the role of *hrcC* in *P. stewartii* subsp. *indologenes* virulence, PNA03-3Δ*hrcC* and PNA14-12Δ*hrcC* were made. Double mutants of *pepM* and *hrcC* were made, using the Δ*pepM* mutant for conjugation, following the deletion procedure as described above.

For the complementation, the *hrcC* gene sequence from PNA03-3 and *pepM* gene sequences from both PNA14-12 and LMG24248, including their native ribosomal binding sites, were PCR-amplified and were used to create pBS46::$hrcC_{03\text{-}3}$/$pepM_{14\text{-}12}$/$pepM_{24248}$ constructs for conjugation with corresponding deletion mutants, following the method described by Stice et al. 2020.

To determine the role of *hal* genes from the Halophos cluster, unmarked deletions of *halA*, *halB*, *halC*, *halD*, *halF*, *halG*, *halH*, *halI*, *halJ*, and *halK* genes in PNA14-12 were made, using the pR6KT2GW allelic exchange vector, following the deletion procedure as described above. The complementations were made as described above for *halB*, *halC*, *halD*, *halF*, *halG*, and *halH* single mutants. In addition, we constructed a plasmid-containing sequence from *halB to halH* and transformed this plasmid pBS46::*halB-H* into onion-nonpathogenic strain *P. stewartii* subsp. *indologenes* PNA15-2.

In planta population and symptomology on onion caused by select *Pantoea* strains.

Pantoea strains (wild types, mutants, and their corresponding complemented strains) were inoculated on leaves and red onion scales as previously described (Stice et al. 2018). Briefly, red onion bulbs (cv. Red Barret) were sliced into small square slices (approximately 2 × 2 cm), were sterilized in 0.5% sodium hypochlorite, and were washed with tap water. A 10-µl pipette tip was used to penetrate the onion scale at the center with finger

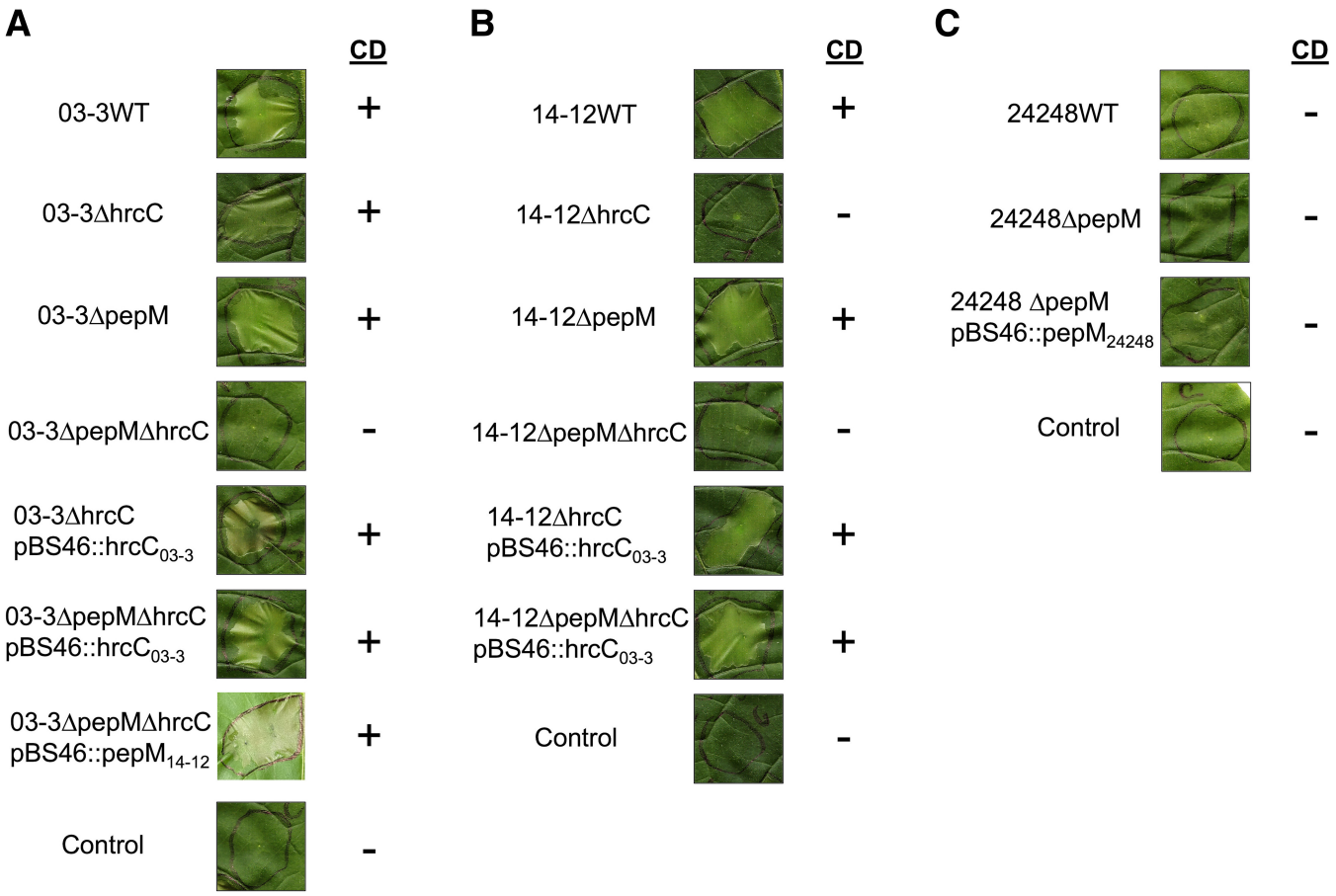

Fig. 8. Tobacco cell-death response to *Pantoea* strains. **A,** *Pantoea stewartii* subsp. *indologenes* 03-3WT, mutants, and selected complemented strains; **B,** *P. stewartii* subsp. *indologenes* 14-12WT, mutants, and selected complemented strains; **C,** *P. allii* 24248WT, mutant, and selected complemented strains. All strains were grown overnight in modified Coplin lab medium (mCLM) at 28°C with shaking. The overnight culture was used to infiltrate panels of tobacco leaves with a blunt-end syringe. Sterile mCLM was used as a control. Tobacco panels were evaluated 48 h postinoculation. Representative images of the cell death response are presented next to our interpretation of the result. The experiment was conducted three times.

pressure. Ten microliters of a 1×10^8 CFU/ml bacterial suspension (1×10^6 CFU) were deposited at the wounded area. The sdH_2O was used as negative control. Samples and images were taken at 4 dpi. Scale tissue samples (approximately 0.2×0.2 cm) were cut, using a sterile blade, 0.5 cm away from the inoculation point, were weighed, and were placed in 2-ml tubes containing three sterile glass beads (3 mm) and 500 µl of sdH_2O. Tissue samples were macerated in a bead mill homogenizer (Omni International Inc, Kennesaw, GA, U.S.A.) four times for 30 s each at a speed of 4 m/s. A 10-fold dilution series of the macerates was made in sdH_2O to 10^{-6} and each dilution was plated as 10-µl droplets on LB agar with rifampicin. Colonies were counted 24 h after incubation and the number was converted to Log_{10} CFUs per gram. Four replicates per strain were used for one experiment and the experiment was conducted at least twice.

Foliage inoculation assays were conducted as described by Koirala et al. (2021). Briefly, onion (cv. Century) seedlings were established in plastic pots and were maintained in a greenhouse at 25 to 30°C. Onion plants about six to eight weeks old were inoculated, after cutting the leaf 1 cm from the apex, with a pair of scissors sterilized with 70% ethanol. Using a micropipette, 10 µl of 1×10^6 CFU/ml bacterial suspension (about 1×10^4 CFU per leaf) was deposited diagonally opposite to each other at the cut end of the leaf twice. Seedlings inoculated with sdH_2O, as described above, were used as negative controls. The strains used in the inoculation included PNA14-12 wild type, PNA03-3 wild type, LMG24248, and their corresponding mutants and complemented strains and are listed in Supplementary Table S2. At 4 dpi, lesion lengths of the inoculated leaf areas were measured. Leaf tissues (0.5 cm long) were taken 0.3 cm away from the inoculation point and were processed similarly to the scale samples, and the enumerated colonies were converted to Log_{10} CFU per square centimeter of leaf area (CFU/cm^2). Four replicates per strain were used for one experiment and the experiment was conducted at least twice.

Symptomology on onion caused by select *Pantoea* strains.

The following South Africa *P. allii* strains, single mutants of *hal* genes and *hal* complemented strains, PNA14-12, PNA15-2, and PNA15-2 pBS46::*halB-H*, were inoculated as described above to compare their symptoms on onion. For both red onion scale assays and foliage inoculation assays, 10 µl of 1×10^6 CFU/ml bacterial suspensions were used. The pictures and lesion lengths were recorded at 5 dpi. Four replicates per strain were used for one experiment and the experiment was conducted twice.

Symptomology on onion leaf caused by culture filtrates of *Pantoea* strains.

We hypothesized that the Halophos gene cluster in *P. stewartii* subsp. *indologenes* PNA14-12 produced a secondary metabolite product, and the product alone could cause symptoms on onion leaves. A single crossover approach similar to that used by Polidore et al. 2021 for in vitro induction of HiVir was used to drive the expression of the Halophos cluster from the rhamnose-inducible P*rhaB* promoter by recombining plasmid pSC201::*halA* before the *halA* gene of the Halophos. The scheme is depicted in Supplementary Figure S3. The first gene, *halA*, in the Halophos gene cluster from PNA14-12, including 39 bp before the start codon, was PCR-amplified, was purified, and was mixed with the plasmid pSC201 (cut with *Xba*I and *Sph*I) in a Gibson-assembly mix (NEB, Ipswich, MA, U.S.A.). The reaction was transformed into *E. coli* DH5α and was plated on LB agar with trimethoprim. The resulting plasmid was confirmed by sequencing and was transformed into *E. coli* RHO5. Bi-parental conjugation was performed by plating a mixture of *E. coli* RHO5 pSC201::*halA* with the PNA14-12 wild type, PNA14-12Δ*pepM*, and PNA14-12Δ*pepM* pBS46::*pepM* on LB agar with DAP. The mixed cultures were streaked onto LB agar with trimethoprim. The single colonies were streaked on LB agar with trimethoprim and were stored. The chromosomal insertion of the plasmid was confirmed by PCR (Supplementary Table S3).

Bacteria were grown in the modified Coplin lab medium (mCLM) (Asselin et al. 2018) at 28°C for 24 h, with shaking at 200 rpm. In order to maintain plasmid insertion, the medium was amended with trimethoprim. For the complemented strain, the medium was also amended with gentamicin. All strains were grown in 5 ml of this broth with and without 0.5% rhamnose. The cultures were centrifuged and the supernatants were filter-sterilized through a 0.2-µm filter to obtain a crude culture filtrate. Before use, 100 µl of this crude culture filtrate was plated on the nutrient agar medium in duplicates to confirm if it was devoid of any bacterial contamination. No colonies were grown after 2 days of incubation at 28°C. Twenty microliters of the crude culture filtrates were inoculated onto the cut end of onion leaf tips as described previously. Inoculated seedlings were assessed for foliar necrosis at 4 dpi and, subsequently, images were taken. The experiments were conducted twice.

In-planta population and symptomology on pearl millet caused by *Pantoea* strains.

We hypothesized that *hrcC* but not *pepM* was important for pearl millet pathogenicity. To determine the role of *pepM* and *hrcC* in the pathogenicity of *P. stewartii* subsp. *indologenes* on pearl millet, *Pantoea* strains were inoculated on 4-week-old pearl millet seedlings (*Pennisetum glaucum* cv. TifGrain 102) at 1×10^6 CFU/ml by syringe infiltration. Pearl millet seedlings were established under the same growth condition as described above for onion seedlings. Symptoms were documented on the inoculated leaves by taking photographs at 4 dpi. In-planta populations of inoculated bacterial strains were assessed at 4 dpi by excising two leaf discs per replicate, using a 0.4 cm diameter cork-borer. Four replicates were sampled per strain and the experiments were conducted twice. Samples were macerated in sdH_2O and were plated on LB agar with rifampicin. Colonies were counted 24 h after incubation and numbers were converted to Log_{10} CFU/cm^2.

Analysis of variance was conducted on Log_{10} CFU/cm^2, Log_{10} CFU/g, and lesion length data, using JMP statistical analysis software (version Pro 16; SAS Institute Inc., Cary, NC, U.S.A.). The effect of strain on the data collected was compared using Tukey-Kramer's honestly significant difference test. The boxplot was generated using the BoxPlotR web tool (Spitzer et al. 2014).

Tobacco infiltration assay.

Pantoea spp. strains were grown overnight in mCLM (Asselin et al. 2018) at 28°C, with shaking at 200 rpm. The following day, overnight cultures (10^8 CFU) were infiltrated into tobacco leaf panels, using a plastic needleless syringe. The infiltrated areas were outlined with a black permanent marker. Sterile mCLM was used as a control. Leaf panels were observed at 24 and 48 h for cell-death responses. The assay was performed on two or three leaves from different plants and was conducted three times.

Identification and analysis of homologous Halophos biosynthetic gene clusters in bacteria.

To assess whether the Halophos gene cluster was introduced by HGT, genomic islands in PNA14-12 were predicted, using IslandViewer 4 (Bertelli et al. 2017). We also computed the GC content, the effective Nc, and the CAI, using CodonW Version 1.4.4 (Peden 1999). In addition, National Center for Biotechnology Information (NCBI) blastn and tblastn were used to identify bacterial genomes that contain Halophos-like gene clusters.

First, the nucleotide sequence of the Halophos gene cluster from PNA14-12 was used to search the NCBI Nucleotide collection database. After identifying Halophos-like gene clusters in several genera, the nucleotide sequence was searched against the NCBI Whole-Genome Shotgun contigs database, by specifying genera *Pantoea*, *Pseudomonas*, *Erwinia*, *Xenorhabdus*, and *Photorhabdus* in the search options. The query coverage and percent identity of the blastn searches were recorded.

In order to show the gene synteny of Halophos-like gene clusters, the PepM protein sequence from PNA14-12 was used as the query in the NCBI blastp search. The NCBI protein accessions of the PepM protein sequences that were in the Halophos-like gene clusters were downloaded and were used as the query in the WebFlaGs web tool (Saha et al. 2021). Results from representative Halophos types of different species were illustrated in PowerPoint, along with a phylogenetic tree based on the corresponding selected PepM protein sequences. Ten PepM protein sequences and *Escherichia coli* 2-methylisocitrate lyase sequence (as an outgroup) were used for multiple sequence alignment, using MAFFT v7.450 (Katoh and Standley 2013) in Geneious Prime 2021.1.1. The alignment was trimmed to the same length and was used for constructing a neighbor-joining tree, using the Jukes-Cantor model (Jukes and Cantor 1969). The bootstrap support values were calculated using 1,000 replicates.

T3SS and T3SE analysis.

Pairwise alignment of *Pantoea stewartii* subsp. *stewartii* DC283 (CP017591) and *P. stewartii* subsp. *indologenes* PNA03-3 (QICO01000005) *hrp*-T3SS genes and surrounding genes was performed in Geneious Prime using MAFFT (Katoh and Standley 2013). The T3SE in strains DC283, PNA03-3, and PNA14-12 were identified by BLAST, using known *Pseudomonas syringae* T3SE sequences listed on figshare (Baltrus and Clark 2019) as queries, and were named based on the closest effector homologs in the NCBI database.

Author-Recommended Internet Resource

T3SE sequence figshare list:
https://figshare.com/s/4e2fdb486d1c31375b52

Literature Cited

Asselin, J. E., Bonasera, J. M., and Beer, S. V. 2018. Center rot of onion (*Allium cepa*) caused by *Pantoea ananatis* requires pepM, a predicted phosphonate-related gene. Mol. Plant-Microbe Interact. 31:1291-1300.

Baltrus, D. A., and Clark, M. 2019. A complete genome sequence for *Pseudomonas syringae* pv. *pisi* PP1 highlights the importance of multiple modes of horizontal gene transfer during phytopathogen evolution. Mol. Plant Pathol. 20:1013-1018.

Bertelli, C., Laird, M. R., Williams, K. P., Simon Fraser University Research Computing Group, Lau, B. Y., Hoad, G., Winsor, G. L., and Brinkman, F. S. L. 2017. IslandViewer 4: Expanded prediction of genomic islands for larger-scale datasets. Nucleic Acids Res. 45:W30-W35.

Blin, K., Shaw, S., Kloosterman, A. M., Charlop-Powers, Z., van Wezel, G. P., Medema, M. H., and Weber, T. 2021. antiSMASH 6.0: Improving cluster detection and comparison capabilities. Nucleic Acids Res. 49:W29-W35.

Brady, C. L., Goszczynska, T., Venter, S. N., Cleenwerck, I., De Vos, P., Gitaitis, R. D., and Coutinho, T. A. 2011. *Pantoea allii* sp. nov., isolated from onion plants and seed. Int. J. Syst. Evol. Microbiol. 61:932-937.

Chang, C. P., Sung, I. H., and Huang, C. J. 2018. *Pantoea dispersa* causing bulb decay of onion in Taiwan. Australas. Plant Pathol. 47:609-613.

Chang, J. H., Desveaux, D., and Creason, A. L. 2014. The ABCs and 123s of bacterial secretion systems in plant pathogenesis. Annu. Rev. Phytopathol. 52:317-345.

Charkowski, A. O. 2007. The soft rot *Erwinia*. Pages 423-505 in: Plant-Associated Bacteria. S.S. Gnanamanickam, ed. Springer, Dordrecht.

Charkowski, A. O., Huang, H. C., and Collmer, A. 1997. Altered localization of HrpZ in *Pseudomonas syringae* pv. *syringae hrp* mutants suggests that different components of the type III secretion pathway control protein translocation across the inner and outer membranes of gram-negative bacteria. J. Bacteriol. 179:3866-3874.

Coplin, D. L., Frederick, R. D., and Majerczak, D. R. 1992a New pathogenicity loci in *Erwinia stewartii* identified by random Tn*5* mutagenesis and molecular cloning. Mol. Plant-Microbe Interact. 5: 266-268.

Coplin, D. L., Frederick, R. D., Majerczak, D. R., and Tuttle, L. D. 1992b. Characterization of a gene cluster that specifies pathogenicity in *Erwinia stewartii*. Mol. Plant-Microbe Interact. 5:81-88.

Coutinho, T. A., and Venter, S. N. 2009. *Pantoea ananatis*: An unconventional plant pathogen. Mol. Plant Pathol. 10:325-335.

De Maayer, P., Chan, W. Y., Rubagotti, E., Venter, S. N., Toth, I. K., Birch, P. R., and Coutinho, T. A. 2014. Analysis of the *Pantoea ananatis* pan-genome reveals factors underlying its ability to colonize and interact with plant, insect and vertebrate hosts. BMC Genomics 15:404.

Edens, D. G., Gitaitis, R. D., Sanders, F. H., and Nischwitz, C. 2006. First report of *Pantoea agglomerans* causing a leaf blight and bulb rot of onions in Georgia. Plant Dis. 90:1551-1551.

Gitaitis, R. D., and Gay, J. D. 1997. First report of a leaf blight, seed stalk rot, and bulb decay of onion by *Pantoea ananas* in Georgia. Plant Dis. 81:1096-1096.

Goettge, M. N., Cioni, J. P., Ju, K.-S., Pallitsch, K., and Metcalf, W. W. 2018. PcxL and HpxL are flavin-dependent, oxime-forming *N*-oxidases in phosphonocystoximic acid biosynthesis in *Streptomyces*. J. Biol. Chem. 293:6859-6868.

Hacker, J., Blum-Oehler, G., Mühldorfer, I., and Tschäpe, H. 1997. Pathogenicity islands of virulent bacteria: Structure, function and impact on microbial evolution. Mol. Microbiol. 23:1089-1097.

Ham, J. H., Majerczak, D., Ewert, S., Sreerekha, M. V., Mackey, D., and Coplin, D. 2008. WtsE, an AvrE-family type III effector protein of *Pantoea stewartii* subsp. *stewartii*, causes cell death in nonhost plants. Mol. Plant Pathol. 9:633-643.

Hattingh, M. J., and Walters, D. F. 1981. Stalk and leaf necrosis of onion caused by *Erwinia herbicola*. Plant Dis. 65:615-618.

Ju, K.-S., Gao, J., Doroghazi, J. R., Wang, K.-K. A., Thibodeaux, C. J., Li, S., Metzger, E., Fudala, J., Su, J., Zhang, J. K., Lee, J., Cioni, J. P., Evans, B. S., Hirota, R., Labeda, D. P., van der Donk, W. A., and Metcalf, W. W. 2015. Discovery of phosphonic acid natural products by mining the genomes of 10,000 actinomycetes. Proc. Natl. Acad. Sci. U.S.A. 112:12175-12180.

Jukes, T. H., and Cantor, C. R. 1969. Evolution of protein molecules. Pages 21-132 in: Mammalian Protein Metabolism. H. N. Munro, ed. Academic Press, New York.

Katoh, K., and Standley, D. M. 2013. MAFFT multiple sequence alignment software version 7: Improvements in performance and usability. Mol. Biol. Evol. 30:772-780.

Koirala, S., Zhao, M., Agarwal, G., Gitaitis, R., Stice, S., Kvitko, B., and Dutta, B. 2021. Identification of two novel pathovars of *Pantoea stewartii* subsp. *indologenes* affecting *Allium* sp. and millets. Phytopathology 111:1509-1519.

Mergaert, J., Verdonck, L., and Kersters, K. 1993. Transfer of *Erwinia ananas* (synonym, *Erwinia uredovora*) and *Erwinia stewartii* to the genus *Pantoea* emend. as *Pantoea ananas* (Serrano 1928) comb. nov. and *Pantoea stewartii* (Smith 1898) comb, nov., respectively, and description of *Pantoea stewartii* subsp. *indologenes* subsp. nov. Int. J. Sys. Bacteriol. 43:162-173.

Peden, J. 1999. Analysis of codon usage. Ph.D. thesis. University of Nottingham, U.K.

Persson, B., Hedlund, J., and Jörnvall, H. 2008. Medium- and short-chain dehydrogenase/reductase gene and protein families: The MDR superfamily. Cell. Mol. Life Sci. 65:3879-3894.

Polidore, A. L. A., Furiassi, L., Hergenrother, P. J., and Metcalf, W. W. 2021. A phosphonate natural product made by *Pantoea ananatis* is necessary and sufficient for the hallmark lesions of onion center rot. MBio 12:e03402-03420.

Roper, M. C. 2011. *Pantoea stewartii* subsp. *stewartii*: Lessons learned from a xylem-dwelling pathogen of sweet corn. Mol. Plant Pathol. 12:628-637.

Saha, C. K., Sanches Pires, R., Brolin, H., Delannoy, M., and Atkinson, G. C. 2021. FlaGs and webFlaGs: Discovering novel biology through the analysis of gene neighbourhood conservation. Bioinformatics 37:1312-1314.

Sharp, P. M., and Li, W. H. 1987. The codon adaptation index—A measure of directional synonymous codon usage bias, and its potential applications. Nucleic Acids Res. 15:1281-1295.

Spitzer, M., Wildenhain, J., Rappsilber, J., and Tyers, M. 2014. BoxPlotR: A web tool for generation of box plots. Nat. Meth. 11:121-122.

Stice, S. P., Stumpf, S. D., Gitaitis, R. D., Kvitko, B. H., and Dutta, B. 2018. *Pantoea ananatis* genetic diversity analysis reveals limited genomic

diversity as well as accessory genes correlated with onion pathogenicity. Front. Microbiol. 9:184.
Stice, S. P., Thao, K. K., Khang, C. H., Baltrus, D. A., Dutta, B., and Kvitko, B. H. 2020. Thiosulfinate tolerance is a virulence strategy of an atypical bacterial pathogen of onion. Curr. Biol. 30:3130-3140.e6.
Stumpf, S., Kvitko, B., Gitaitis, R., and Dutta, B. 2018. Isolation and characterization of novel *Pantoea stewartii* subsp. *indologenes* strains exhibiting center rot in onion. Plant Dis. 102:727-733.
Wright, F. 1990. The 'effective number of codons' used in a gene. Gene. 87:23-29.
Xin, X. F., Kvitko, B., and He, S. Y. 2018. *Pseudomonas syringae*: What it takes to be a pathogen. Nat. Rev. Microbiol. 16:316-328.
Zhang, Y., Chen, L., Wilson, J. A., Cui, J., Roodhouse, H., Kayrouz, C., Pham, T. M., and Ju, K.-S. 2022. Valinophos reveals a new route in microbial phosphonate biosynthesis that Is broadly conserved in nature. J. Am. Chem. Soc. 144:9938-9948.